Supporting Information for

Redox Active Mixed-Valence Hexamanganese Double-cubane Complexes Supported by Tetravanadates

Tatsuya Maruyama,[a] Akimi Namekata,[a] Hiroshi Sakiyama,[b] Yuji Kikukawa,[a] Yoshihito Hayashi*[a]

a Department of Chemistry, Graduate School of Natural Science and Technology, Kanazawa University, Kakuma, Kanazawa 920-1192, Japan

E-mail: hayashi@se.kanazawa-u.ac.jp

b Department of Science, Faculty of Science, Yamagata University, Kojirakawa, Yamagata 990-8560, Japan

Contents

assignment of peaks.

Figure S4. Positive-ion CSI-MS spectrum of **1(*p*-ClPhCO$_2$)** in acetonitrile. The table shows the assignment of peaks.

Figure S5. Positive-ion CSI-MS spectrum of **1(*p*-NO$_2$PhCO$_2$)** in acetonitrile. The table shows the assignment of peaks.

Figure S6. Positive-ion CSI-MS spectrum of **2(*o*-MePhCO$_2$)** in acetonitrile. The table shows the assignment of peaks.

Figure S7. Positive-ion CSI-MS spectrum of **2(*p*-MePh)** in acetonitrile. The table shows the assignment of peaks.

Figure S8. UV-Vis-NIR spectra of **1(*p*-MePhCO$_2$)** (black line) and **2(*p*-MePhCO$_2$)** (red line) in acetonitrile (2.0×10^{-5} M).

Figure S9. Cyclic voltammograms of (a) **1(MeCO$_2$)**, (b) **1(*p*-MeOPhCO$_2$)**, (c) **1(PhCO$_2$)**, (d) **1(*p*-MePhCO$_2$)**, (e) **1(*p*-ClPhCO$_2$)**, (f) **1(*p*-NO$_2$PhCO$_2$)**, (g) **2(*p*-MePhCO$_2$)**, and **2(*o*-MePhCO$_2$)** in acetonitrile. Scan rate was 100 mV/s. The working electrode was glassy carbon and the reference electrode was the Ag/Ag$^+$ electrode. The supporting electrolyte was (n-Bu$_4$N)PF$_6$.

Figure S10. (a) Cyclic voltammograms of **1(*p*-MePhCO$_2$)** in acetonitrile in the presence of 0, 1, 2, 4, 6, 8 eq. of *p*-MePhCO$_2$H. (b) Plots of the eq. of *p*-MePhCO$_2$H added to **1(*p*-MePhCO$_2$)** versus the observed open circuit potential (E_{OCP}) of **1(*p*-MePhCO$_2$)** in the presence of *p*-MePhCO$_2$H.

Figure S11. Temperature dependence of $\chi_{\mathrm{M}}T$ values of (a) **1(MeCO$_2$)**, (b) **1(PhCO$_2$)**, (c) **1(*p*-ClPhCO$_2$)**, (d) **1(*p*-MePhCO$_2$)**, (e) **1(*p*-NO$_2$PhCO$_2$)**, (f) **2(*p*-MePhCO$_2$)**, and (g) **2(*o*-MePhCO$_2$)** in the temperature range of 2–300 K under the magnetic field of 1000 Oe. Solid lines represents the best fits.

Figure S12. Magnetic coupling scheme for (a) the **2(RCO$_2$)** complexes at 300 K, (b) **2(*o*-MePhCO$_2$)** at 2 K, and (c) **2(*p*-MePhCO$_2$)** at 2 K.

Figure S13. Thermogravimetric analysis of (a) **1($MeCO_2$)**, (b) **1($PhCO_2$)**, (c) **1(*p*-$MePhCO_2$)**, (d) **1(*p*-$MeOPhCO_2$)**, (e) **1(*p*-$ClPhCO_2$),** (f) **1(*p*-NO_2PhCO_2)**, (g) **2(*p*-$MePhCO_2$)**, and (h) **2(*o*-$MePhCO_2$)**.

Table S1. Reported Manganese Containing Polyoxometalates

Compound	The number of Mn^{n+} ions	Ref.
$[XMn^{II}W_{11}O_{40}H_2]^{n-}$ (X = B, Zn, P, Si, Ge)	1	S1
$[XMn^{III}W_{11}O_{40}H_2]^{n-}$ (X = B, Zn, P, Si, Ge)	1	S1
$[XMn^{II}Mo_{11}O_{40}H_2]^{n-}$ (X = P, Si, Ge)	1	S1
$K_7[Mn^{III}(H_2O)P_2W_{11}O_{61}]$	1	S2
$(n\text{-}Bu_4N)_{7.3}H_{0.7}[Mn^{III}BrP_2W_{11}O_{61}]$	1	S2
$(NH_4)_4[Mn^{IV}XMo_{12}O_{42}]$ (X = U, Th)	1	S3
$A_7[XMn^{IV}W_{11}O_{40}H]$ (A = K, Cs, TBA[a], THA[b]; X = Zn, B, Si)	1	S4
α-$K_{9-n}[AlMn^{n+}W_{11}O_{39}]$ (n = 2–4)	1	S5
$Rb_8[As_2Mn^{II}W_{20}O_{68}]$	1	S6
$TBA_3[Mn^{III}Mo_6O_{18}(C_4H_6O_3NO_2)(C_4H_6O_3NH_2)]$	1	S7
$TBA_5[Mn^{III}(N_3)PW_{11}O_{39}]$	1	S8
$TBA_5[\{Mn^{V}N\}PW_{11}O_{39}]$	1	S8
$TBA_3[Mn^{III}Mo_6O_{18}((OCH_2)_3)CN{=}CHC_6H_4(B(OR)_2)_2]$ (R = H, Me)	1	S9
$TBA_3[Mn^{III}Mo_6O_{18}((OCH_2)_3)CN{=}CHC_6H_4(BO_2(CH_2)_3)_2]$	1	S9
$TBA_3[Mn^{III}Mo_6O_{18}\{(OCH_2)_3CNHCOR\}_2]$ (R = C_6H_5, C_8H_7)	1	S10
$(C_{16}H_{36}N)[MnMo_6O_{18}((OCH_2)_3C\text{-}NH\text{-}CO\text{-}CH_2\text{-}Cl)_2]$	1	S11
$TBA_5[Mo_6O_{18}NC(OCH_2)_3Mn^{III}Mo_6O_{18}(OCH_2)_3CNH_2]$	1	S12
$K_{16}[NaH_2Mn^{II}W_{17}F_6O_{55}]_2$	1	S13
$K_8[NaH_2Mn^{III}(H_2O)W_{17}F_6O_{55}]$	1	S13
$K_{12\text{-}n}[NaH_2Mn^{n+}(OH)W_{17}F_6O_{55}]$ (n = 4, 5)	1	S13
$TBA_7H_{10}[Mn^{III}(A\text{-}\alpha\text{-}SiW_9O_{34})_2]$	1	S14
$[Na(H_2O)_5](NH_4)_7[P_2W_{15}O_{56}Co_3(H_2O)_3(OH)_3Mn^{I}(CO)_3]$	1	S15
$X_7[MnV_{13}O_{38}]$ (X = K, Na, NH_4, Li)	1	S16
$K_5[MnV_{11}O_{32}]$	1	S17
$X_{4.5}H_{0.5}[MnV_{11}O_{32}]$ (X = Cs, NH_4)	1	S17
$K_4Li_2[Mn^{IV}V_{14}O_{40}]$	1	S18
$TBA_3[DMA^{c}(MnCl)V_{12}O_{32}Cl]$	1	S19
$TBA_4[PW_{11}O_{39}M^{III}OH_2]$	1	S20
$TMA^{d}{}_8[H_2Mn^{IV}Nb_{10}O_{32}]$	1	S21
$(NH_4)_{10}[Mn(H_2O)_4(P_2Mo_5O_{23})_2]$	1	S22
K9Na2[HMn(Nb6O19)2]	1	S23
$Na_{14-n}[WZnMn^{n+}{}_2(ZnW_9O_{34})_2]$ (n = 2, 3)	2	S24
$A_4[H_6SiMn^{III}{}_2W_{10}O_{40}]$ (A = TBA, $(CH_3)_3PhN$)	2	S25
$TBA_{3.5}H_{5.5}[SiMn^{III}Mn^{IV}W_{10}O_{40}]$	2	S25
$K_6[H_6SiMn_2W_{10}O_{40}]$	2	S25
$K_4Na_6Mn[\{SiMn^{II}{}_2W_9O_{34}(H_2O)\}_2]$	2	S26
$Na_{17}[Ni_4Mn^{II}{}_2P_3W_{24}O_{94}(H_2O)_2]$	2	S27

Table S1. Reported Manganese Containing Polyoxometalates (continue)

Compound	The number of Mn^{n+} ions	Ref.
$TEA^e{}_6TBA_2H_2[\{(\gamma\text{-}SiW_{10}O_{36})Mn^{III}{}_2(OH)_2(N_3)_{0.5}(H_2O)_{0.5}\}_2(\mu\text{-}1,3\text{-}N_3)]$	2	S28
$[FeMn^{n+}{}_2(H_2O)_2(FeW_9O_{34})_2]^{(16-2n)-}$ (n = 2, 3)	2	S29
$K_6[Mn^{III}{}_2SiW_{10}O_{37}(OH)(H_2O)]$	2	S30
$K_{10}[Mn^{IV}{}_2V_{22}O_{64}]$	2	S31
$TBA_4[(MnCl)_2V_{12}O_{32}Cl]$	2	S19
$Na_{14-n}[WMn^{n+}{}_3(ZnW_9O_{34})_2]$ (n = 2, 3)	3	S24
$Cs_4K_{11}[(\beta_2\text{-}SiW_{11}Mn^{II}O_{38}OH)_3]$	3	S32
$K_{11}Na[As_2W_{18}\{Mn^{II}(H_2O)\}_3O_{66}]$	3	S33
$TMA_4Na_7[(Mn^{III}(H_2O))_3(SbW_9O_{33})_2]$	3	S34
$Na_{8.25}[(Mn^{III}(H_2O))_{2.25}(WO(H_2O))_{0.75}(AsW_9O_{33})_2]$	3	S34
$Na_3K_9[Mn^{II}(H_2O)Mn_2(AsW_9O_{33})_2]$	3	S34
$Na_2K_{11}H_3[Mn^{II}Mn^{III}{}_2(H_2O)_3SiW_9O_{37}]_2$	3	S35
$K_6Cs[C(NH_2)_3]_2[Mn^{III}{}_3(H_2O)_5(A\text{-}a\text{-}PW_9O_{34})_2]$	3	S36
$K_5H_3[Mn^{IV}{}_3V_{12}O_{40}]$	3	S37
$X_5[HMn_3V_{12}O_{39}]$ (X = K, NH_4)	3	S17
$Na_{2.5}K_{4.5}[Mn^{II}{}_3(OH)_3(H_2O)_3(A\text{-}\alpha\text{-}SiW_9O_{34})]$	3	34
$K_4[Mn^{III}{}_3(OH)_3(H_2O)_3(A\text{-}\alpha\text{-}SiW_9O_{34})]$	3	34
$NaK_3[Mn^{III}{}_3(OH)_3(H_2O)_3(A\text{-}\beta\text{-}SiW_9O_{34})]$	3	34
$K_4[Mn^{III}{}_4(OH)_3(H_2O)_3SiW_9O_{34}]$	4	S34
$Na_{16}[Mn^{II}{}_4(H_2O)_2(P_2W_{15}O_{56})_2]$	4	S38
$K_{10}[Mn^{II}{}_4(H_2O)_2(PW_9O_{34})_2]$	4	S39
$K_9[Mn^{III}Mn^{II}{}_3(H_2O)_2(PW_9O_{34})_2]$	4	S39
$K_{1.5}Cs_{7.5}[Mn^{III}{}_3Mn^{II}(OH)_2(PW_9O_{34})_2]$	4	S39
$DMA_{5.33}H_2Mn^{II}{}_{0.33}[(\alpha\text{-}P_2W_{15}O_{56})Mn^{III}{}_3Mn^{IV}O_3(OAc^f)_3]$	4	35
$KnNa_6[\{XMn^{III}{}_4(\mu_3\text{-}O)_2(\mu_2\text{-}OH)_2(H_2O)(CO_3)\}(\beta\text{-}SiW_8O_{31})_2]$ (X = Dy^{3+}: n = 7, X = K^+: n = 9)	4	S40
$TBA_7[FeMn^{III}{}_4\{Ln(C_5H_7O_2)\}_2O_2(SiW_9O_{34})_2]$ (Ln = Gd, Dy)	4	S41
$(H_2en^g)_8Na(H_2O)_2H[H_{16}\{[Mn^{II}(OH)_2]_2W_7O_{32}\}\{Ag_4O_3[Mn^{II}(OH_2)]_2\}(SbW_9O_{33})]_2$	4	S42
$K_5Mn_{0.5}[\{Ln(H_2O)_6\}_2Mn^{II}{}_4(B\text{-}\alpha\text{-}SiW_9O_{34})_2(H_2O)_2]$ (Ln = La, Nd)	4	S43
$K_5Mn[\{Ln(H_2O)_5\}_2Mn^{II}{}_4(B\text{-}\alpha\text{-}SiW_9O_{34})_2(H_2O)_2]$ (Ln = Gd, Dy, Er)	4	S43
$K_8MnH_2[Mn^{II}{}_4(B\text{-}\alpha\text{-}SiW_9O_{34})_2(H_2O)_2]$	4	S43
$K_{18}[\{Mn^{II}(H_2O)_3\}_2\{Mn^{II}(H_2O)_2\}\{Mn^{II}{}_3(B\text{-}\alpha\text{-}SiW_8O_{30}(OH))(B\text{-}\beta\text{-}SiW_9O_{33}(OH)(H_2O))_2]$	4	S43
$TBA_3[Mn^{III}{}_2Mn^{IV}{}_2V_4O_{17}(OAc)_3]$	4	S44
$Na_{10}(H_2O)_{42}[\{Dy(H_2O)_6\}_2\{Mn_4(H_2O)_2(P_2W_{15}O_{56})_2\}]$	4	S45
$Na_x[\{Mn^{II}(bpy)\}_2Na(H_2O)_2(Mn^{II}Cl)_n\{Mn^{II}(H_2O)\}_m(XW_9O_{33})_2]$ (x = 9, n =2, m = 1 for X = As, x = 8, n = 1, m = 2 for X = Sb)	5	S46
$[\{Gd(H_2O)_8\}_4\{Mn^{II}(H_2O)_5\}_2\{Mn^{II}{}_4(H_2O)_2P_4W_{30}O_{112}\}]$	6	S47

Table S1. Reported Manganese Containing Polyoxometalates (continue)

Compound	The number of Mn^{n+} ions	Ref.
$Na_4K(C_4H_{10}NO)_7\{[GeW_9O_{34}]_2[Mn^{III}_4Mn^{II}_2O_4(H_2O)_4]\}$	6	36
$(C_4H_{10}NO)_{12}\{[SiW_9O_{34}]_2[Mn^{III}_4Mn^{II}_2O_4(H_2O)_4]\}$	6	36
$Na_{17}[Mn_6P_3W_{24}O_{94}(H_2O)_2]$	6	S48
$DMA_6H_2[\{\alpha\text{-}P_2W_{16}O_{57}(OH)_2\}\{Ce^{IV}Mn^{IV}_6O_9(OAc)_8\}]$	6	S49
$Rb_{11}K_6[Rb\subset(GeW_{10}Mn^{III}_2O_{38})_3]$	6	S50
$Na_{10}H_8[Mn^{II}_4Mn^{III}_2Ge_3W_{24}O_{94}(H_2O)_2]$	6	S51
$K_{18}[Mn^{III}_2Mn^{II}_4(\mu_3\text{-}O)(H_2O)_4(B\text{-}\beta\text{-}SiW_8O_{31})(B\text{-}\beta\text{-}SiW_9O_{34})(\gamma\text{-}SiW_{10}O_{36})]$	6	S52
$Na_{11}Li_{12}[Mn^{II}_6(PW_6O_{26})(\alpha\text{-}P_2W_{15}O_{56})_2(H_2O)_2]$	6	S53
$(H_3deta^{h})_4[(B\text{-}\alpha\text{-}SiW_9O_{34})_2Mn^{III}_4Mn^{II}_2O_4(H_2O)_4]$	6	S54
$[H_2en]_5[(B\text{-}\alpha\text{-}SiW_9O_{34})_2Mn^{III}_4Mn^{II}_2O_4(H_2O)_2(Hen)_2]$	6	S54
$[H_2ppz^{i}]_4[H_21,3\text{-}dap^{j}]_2[(B\text{-}a\text{-}SiW_9O_{34})_2Mn^{III}_4Mn^{II}_2O_4(H_2O)_2(ppz)_2]$	6	S54
$H_2[H_2ppz]_4[(B\text{-}\alpha\text{-}SiW_9O_{34})_2Mn^{III}_4Mn^{II}_2O_4(H_2O)_2(Hppz)_2]$	6	S54
$[H_2ppz]_3[H_3deta]_2[(B\text{-}a\text{-}SiW_9O_{34})_2Mn^{III}_4Mn^{II}_2O_4(ppz)_4]$	6	S54
$[H_2ppz]_2[H_2en]_2[(B\text{-}a\text{-}SiW_9O_{34})_2Mn^{III}_4Mn^{II}_2O_4(Hppz)_4]$	6	S54
$Na_{36}K_{11}[\{a\text{-}P_2W_{15}O_{56}\}_6\{Ce_3Mn_2(\mu_3\text{-}O)_4(\mu_2\text{-}OH)2\}_3(\mu_2\text{-}OH)_2(H_2O)_2(PO_4)]$	6	S55
$Na_{14}[(\alpha\text{-}P_2W_{15}O_{56})_2Mn^{III}_6Mn^{IV}O_6(H_2O)_6]$	7	S56
$K_{22}[Mn(H_2O)_2\{Mn_3(H_2O)(B\text{-}\beta\text{-}GeW_9O_{33}(OH))(B\text{-}\beta\text{-}GeW_8O_{30}(OH))\}_2]$	7	S57
$K_{18}[Mn^{II}_2\{Mn^{II}(H_2O)_5Mn^{III}_3(H_2O)(B\text{-}b\text{-}SiW_9O_{34})(B\text{-}b\text{-}SiW_6O_{26})\}_2]$	8	S58
$Na_5Li_{20}[W_{40}Mn^{II}_9P_8O_{174}(OH)_5(H_2O)_6]$	9	S53
$K_{14}Na_8[Mn^{III}_6Mn^{IV}_4O_4(OH)_{12}(H_2O)_{12}(A\text{-}\beta\text{-}AsW_9O_{34})_4]$	10	S59
$(C_4H_{10}NO)_{40}[W_{72}Mn_{12}^{III}O_{268}X_7]$ (X = Si, Ge)	12	S60
$K_{14}Na_{17}[(Mn^{III}_{13}Mn^{II})O_{12}(PO_4)_4(PW_9O_{34})_4]$	14	S61
$Na_4H_8DMA_{14}[\{Mn^{III}_3Mn^{IV}_4O_4(OH)_2(OH_2)\}_2(W_6O_{22})(H_2W_8O_{32})_2(H_4W_{13}O_{46})_2]$	14	S62
$K_{10}[H_{31}(Nb_6P_2W_{12}O_{62})_6\{Mn^{III}_3(OH)_3(H_2O)_6\}_4\{Mn^{II}_{0.75}Na_{0.25}(H_2O)_4\}_4]$	15	S63
$Na_{19.5}Cs_{8.5}[\{Mn^{III}_{10}Mn^{II}_6O_6(OH)_6(PO_4)_4\}(A\text{-}\alpha\text{-}SiW_9O_{34})_4]$	16	S64
$Na_{18}Rb_{10}[\{Mn^{III}_4Mn^{II}_{12}(OH)_{12}(PO_4)_4\}(A\text{-}\alpha\text{-}SiW_9O_{34})_4]$	16	S64
$Na_{34}[Mn^{II}_{19}(OH)_{12}(SiW_{10}O_{37})_6]$	19	S65
$TBA_{24}[\{\gamma\text{-}P_2W_{12}O_{48}Mn^{II}_4(H_2O)_6\}_4(H_2O)_4]$	16	S66
$TBA_{42}[\{\gamma\text{-}P_2W_{12}O_{48}Mn^{III}_2Mn^{II}_2(acac^{k})_2(OAc)\}_6]$	24	S66
$K_{56}Li_{74}H_{14}[Mn^{III}_{40}P_{32}W_{224}O_{888}]$	40	S67

a. TBA = tetrabutylammonium, b. THA = tetrahexylammonium, c. DMA = dimethylammonium, d = tetramethylammonium, e = tetraethylammonium, f. OAc = acetate, g. en = ethylenediamine, h. diethylenetriamine, i = piperazine, j = diaminopropane, k. acac = acetylacetonate.

Table S2. Crystallographic Data of **1(MeCO$_2$)**, **1(PhCO$_2$)**, **1(*p*-MePhCO$_2$)**, **1(*p*-ClPhCO$_2$)**, **1(*p*-NO$_2$PhCO$_2$)**, **2(*p*-MePhCO$_2$)**, and **2(*o*-MePhCO$_2$)**

	1(MeCO$_2$)	**1(PhCO$_2$)**	**1(*p*-MePhCO$_2$)**	**1(*p*-ClPhCO$_2$)**
formula	$C_{52}H_{130}Mn_6N_6O_{38}V_8$	$C_{70}H_{154}Mn_6N_{14}O_{52}V_8$	$C_{69}H_{149}Mn_6N_{11}O_{47}V_8$	$C_{72}H_{154}Cl_2Mn_6N_{16}O_{56}V_8$
fw	2184.77	2751.22	2622.14	2948.16
crystal system	monoclinic	monoclinic	triclinic	monoclinic
space group	$P2_1/c$ (no.14)	$P2_1/c$ (no.14)	$P-1$ (no.2)	$P2_1/c$ (no.14)
a (Å)	14.4163 (3)	15.1262 (4)	14.8347 (4)	15.2732 (7)
b (Å)	24.0448 (5)	16.2033 (4)	14.9350 (4)	16.3157 (7)
c (Å)	13.6611 (3)	24.7209 (6)	26.9416(6)	24.4982 (11)
α (deg)	90	90	84.8770 (10)	90
β (deg)	116.8570 (10)	99.968 (1)	88.8120 (10)	6053.1 (5)
γ (deg)	90	90	65.6960 (10)	90
V (Å^3)	4224.66 (16)	5967.5 (3)	5417.5 (2)	6053.1 (5)
Z	2	2	2	2
temp. (K)	90 (2)	90 (2)	90 (2)	90 (2)
GOF	0.990	1.029	1.031	1.029
$R1$ [$I > 2\sigma(I)$]	0.0353	0.0693	0.0501	0.0712
$wR2$ [$I > 2\sigma(I)$]	0.0804	0.2197	0.1408	0.2019

$R1 = \sum||F_o| - |F_c|/\sum|F_o|$. $wR2 = \{\sum[w(F_o^2 - F_c^2)]/ \sum[w(F_o^2)^2]\}^{1/2}$.

Table S2. Crystallographic Data of **1(MeCO$_2$)**, **1(PhCO$_2$)**, **1(*p*-MePhCO$_2$)**, **1(*p*-ClPhCO$_2$)**, **1(*p*-NO$_2$PhCO$_2$)**, **2(*p*-MePhCO$_2$)**, **and 2(*o*-MePhCO$_2$)** (continue)

	1(*p*-NO$_2$PhCO$_2$)	**2(*p*-MePhCO$_2$)**	**2(*o*-MePhCO$_2$)**
formula	$C_{34}H_{73}Mn_3N_7O_{26}V_4$	$C_{57.5}H_{118.5}Mn_6N_{6.5}O_{39}V_8$	$C_{56}H_{114}Mn_6N_5O_{36}V_8$
fw	1364.57	2262.24	2170.68
crystal system	monoclinic	triclinic	monoclinic
space group	$P2_1/c$ (no. 14)	$P1$ (no. 1)	$P2_1/c$ (no. 14)
a (Å)	15.2949 (4)	13.2975 (4)	14.2609 (3)
b (Å)	16.3939 (4)	19.0223 (5)	24.8229 (5)
c (Å)	24.2876 (6)	20.3933 (6)	13.5776 (3)
α (deg)	90	81.7410 (10)	90
β (deg)	96.3330 (10)	72.9210 (10)	117.4990 (10)
γ (deg)	90	73.9560 (10)	90
V (Å^3)	6052.8 (3)	4727.9 (2)	4263.69 (16)
Z	4	2	2
temp. (K)	90 (2)	90 (2)	90 (2)
GOF	1.063	1.052	1.034
$R1$ [$I > 2\sigma(I)$]	0.0620	0.0699	0.0490
$wR2$ [$I > 2\sigma(I)$]	0.1912	0.2015	0.1261

$R1 = \sum||F_o| - |F_c|/\sum|F_o|$. $wR2 = \{\sum[w(F_o^2 - F_c^2)]/ \sum[w(F_o^2)^2]\}^{1/2}$.

Table S3. Selected BVS Values of **1(RCO$_2$)** and **2(RCO$_2$)**

	1(MeCO$_2$)		**1(PhCO$_2$)**		**1(*p*-ClPhCO$_2$)**		**1(*p*-NO$_2$PhCO$_2$)**	
	Mn^{3+}	Mn^{4+}	Mn^{3+}	Mn^{4+}	Mn^{3+}	Mn^{4+}	Mn^{3+}	Mn^{4+}
Mn1	3.15	3.09	3.34	3.28	3.45	3.38	3.24	3.17
Mn2	3.09	3.03	3.12	3.06	3.13	3.07	3.10	3.04
Mn3	3.85	3.77	3.80	3.73	3.63	3.57	3.87	3.80

	1(*p*-MePhCO$_2$)		**2(*p*-MePhCO$_2$)**		**2(*o*-MePhCO$_2$)**	
	Mn^{3+}	Mn^{4+}	Mn^{3+}	Mn^{4+}	Mn^{3+}	Mn^{4+}
Mn1	3.09	3.03	3.86	3.79	4.02	3.95
Mn2	3.24	3.18	3.20	3.14	3.13	3.07
Mn3	3.81	3.74	3.80	3.73	3.58	3.51
Mn4	3.13	3.07	3.62	3.55	-	-
Mn5	3.30	3.24	3.97	3.89	-	-
Mn6	3.67	3.60	3.12	3.06	-	-
Mn7	-	-	3.91	3.84	-	-
Mn8	-	-	3.10	3.04	-	-
Mn9	-	-	3.91	3.84	-	-
Mn10	-	-	3.96	3.88	-	-
Mn11	-	-	3.47	3.40	-	-
Mn12	-	-	3.27	3.21	-	-

Table S4. Selected Bond Lengths (Å) and Angels (deg) for **1(RCO$_2$)** and **2(*o*-MePhCO$_2$)** (Left; R = Me, Ph, *p*-ClPh, *p*-NO$_2$Ph, *p*-MePh) and **2(*p*-MePhCO$_2$)** (right)

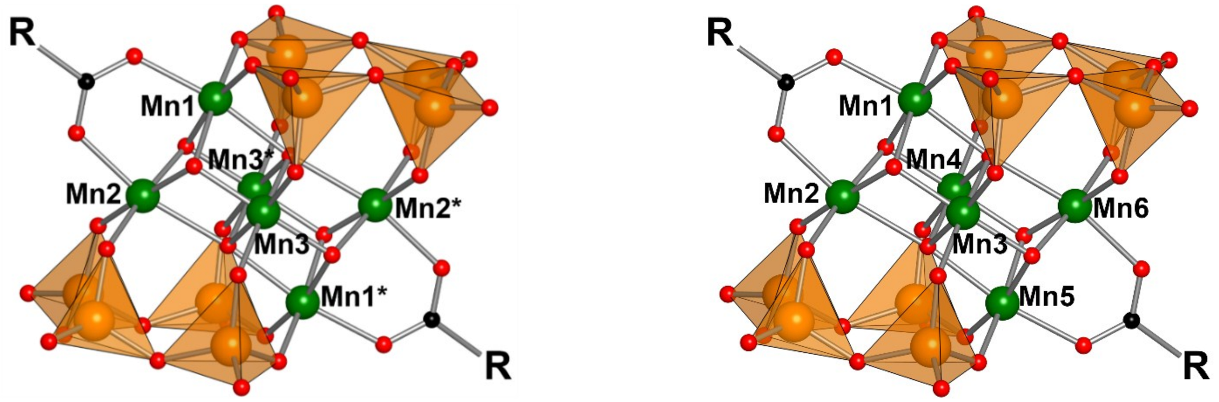

	1(MeCO$_2$)	**1(PhCO$_2$)**	**1(*p*-ClPhCO$_2$)**	**1(*p*-NO$_2$PhCO$_2$)**	**2(*o*-MePhCO$_2$)**
Bond Lengths (Å)					
Mn1···Mn2	2.8337	2.843	2.846	2.8537	2.841
Mn1···Mn3	2.9825, 2.9996	2.950, 2.976	3.069, 3.040	2.9651, 2.978	2.9165, 2.884
Mn2···Mn3	3.0639, 3.0722	3.043, 3.059	2.976, 2.928	3.0467, 3.035	3.1326, 3.1167
Mn3···Mn3*	2.8729	2.926	2.991	2.906	3.0533
Mn^{3+}–O_{axial}	2.151–2.318	2.109–2.298	2.073–2.298	2.129–2.273	2.162–2.440
Mn^{3+}–$O_{equatrial}$	1.909–1.953	1.908–1.937	1.907–1.936	1.914–1.948	1.911–1.922
Mn^{4+}–O	1.912–1.939	1.903–1.985	1.905–2.055	1.899–1.957	1.881–1.949
Bond Angles (deg)					
Mn1–O–Mn2	94.72, 94.97	95.3, 95.7	95.6, 95.9	95.3, 95.7	95.7, 95.7
Mn1–O–Mn3	92.07, 100.7	93.5, 99,8	92.3, 100.7	92.6, 100.6	95.5, 97.6
Mn1–O–Mn3*	92.75, 101.5	92.6, 100.7	94.3, 98.9	93.0, 100.4	94.2, 99.1
Mn2–O–Mn3	92.03, 105.5	90.9, 105.6	91.8, 104.8	92.3, 104.6	87.8, 109.0
Mn2–O–Mn3*	92,36, 106.0	91.9, 104.8	89.5, 105.9	91.8, 104.7	89.1, 108.8
Mn3–O–Mn3*	96.6	97.2	97.6	97.1	98.2

Table S4. Selected Bond Lengths (Å) for **1(RCO$_2$)** and **2(RCO$_2$)** (continue)

1(*p*-MePhCO$_2$)		**2(*p*-MePhCO$_2$)**			
Bond Lengths (Å)		Bond Lengths (Å)		Bond Angles (deg)	
Mn1···Mn2	2.8431	Mn1···Mn2	2.846	Mn1–O–Mn2	94.9, 95.6
Mn1···Mn3	3.0433, 3.0554	Mn1···Mn3(4)	2.922, 2.892	Mn1–O–Mn3	94.6, 99.4
Mn2···Mn3	2.9716, 2.9786	Mn2···Mn3(4)	3.105, 3.106	Mn1–O–Mn4	94.3, 98.3
Mn3···Mn3*	2.9278	Mn3···Mn4	3.033	Mn2–O–Mn3	89.6, 110.0
Mn4···Mn5	2.8585	Mn3···Mn5(6)	2.880, 3.100	Mn2–O–Mn4	86.7, 109.3
Mn4···Mn6	3.0343, 3.0483	Mn4···Mn5(6)	2.932, 3.097	Mn3–O–Mn4	99.1, 97.0
Mn5···Mn6	2.9829, 2.9609	Mn5···Mn6	2.846	Mn3–O–Mn5	96.0, 96.8
Mn6···Mn6*	2.9992	Mn7···Mn8	2.848	Mn3–O–Mn6	89.2, 106.9
Mn^{3+}–O_{axial}	2.108–2.277	Mn7···Mn9(10)	2.901, 2.896	Mn4–O–Mn5	94.1, 99.3
Mn^{3+}–$O_{equatrial}$	1.912–1.951	Mn8···Mn9(10)	3.092, 3.084	Mn4–O–Mn6	89.9, 105.7
Mn^{4+}–O	1.917–2.015	Mn9···Mn10	2.939	Mn5–O–Mn6	95.5, 96.2
		Mn9···Mn11(12)	2.965, 3.105	Mn7–O–Mn8	95.3, 94.6
Bond Angles (deg)		Mn10···Mn11(12)	2.956, 3.103	Mn7–O–Mn9	95.8, 99.4
Mn1–O–Mn2	94.8, 95.1	Mn11···Mn12	2.840	Mn7–O–Mn10	95.2, 98.2
Mn1–O–Mn3	92.1, 105,3	Mn^{3+}–O_{axial}	2.119–2.442	Mn8–O–Mn9	90.8, 108.3
Mn1–O–Mn3*	92.0, 104.8	Mn^{3+}–$O_{equatrial}$	1.890–1.943	Mn8–O–Mn10	91.0, 107.0
Mn2–O–Mn3	92.4, 100.7	Mn^{4+}–O	1.870–1.990	Mn9–O–Mn10	97.2, 98.3
Mn2–O–Mn3*	92.7, 100.4			Mn9–O–Mn11	93.8, 99.8
Mn3–O–Mn3*	97.4			Mn9–O–Mn12	89.2, 108.1
Mn4–O–Mn5	96.0, 95.5			Mn10–O–Mn11	94.0, 99.5
Mn4–O–Mn6	90.8, 105.2			Mn10–O–Mn12	88.8, 107.3
Mn4–O–Mn6*	91.8, 104.5			Mn11–O–Mn12	96.2, 95.8
Mn5–O–Mn6	93.4, 100.1				
Mn5–O–Mn6*	92.6, 101.1				
Mn6–O–Mn6*	98,0				

Table S5. The best fitting parameters for **1(RCO$_2$)** and **2(RCO$_2$)**

	1(MeCO$_2$)	**1(PhCO$_2$)**	**1(*p*-ClPhCO$_2$)**	**1(*p*-MePhCO$_2$)**	**1(*p*-NO$_2$PhCO$_2$)**	**2(*o*-MePhCO$_2$)**	**2(*p*-MePhCO$_2$)**
J	6.6 cm^{-1}	3.0 cm^{-1}	1.9 cm^{-1}	0.83 cm^{-1}	6.2 cm^{-1}	−7.0 cm^{-1}	−15 cm^{-1}
J'	−54 cm^{-1}	−43 cm^{-1}	−50 cm^{-1}	−50 cm^{-1}	−61 cm^{-1}	-	10 cm^{-1}
J''	8.2 cm^{-1}	2.8 cm^{-1}	3.8 cm^{-1}	1.5 cm^{-1}	9.4 cm^{-1}	-	-
TIP	3.5×10^{-4} cm^3 mol^{-1}	3.5×10^{-4} cm^3 mol^{-1}	3.5×10^{-4} cm^3 mol^{-1}	3.5×10^{-4} cm^3 mol^{-1}	3.5×10^{-4} cm^3 mol^{-1}	4.1×10^{-4} cm^3 mol^{-1}	4.1×10^{-4} cm^3 mol^{-1}
θ	0 cm^{-1}	−0.83 cm^{-1}	−1.7 cm^{-1}	−0.91 cm^{-1}	−0.44 cm^{-1}	0 cm^{-1}	−0.10 cm^{-1}

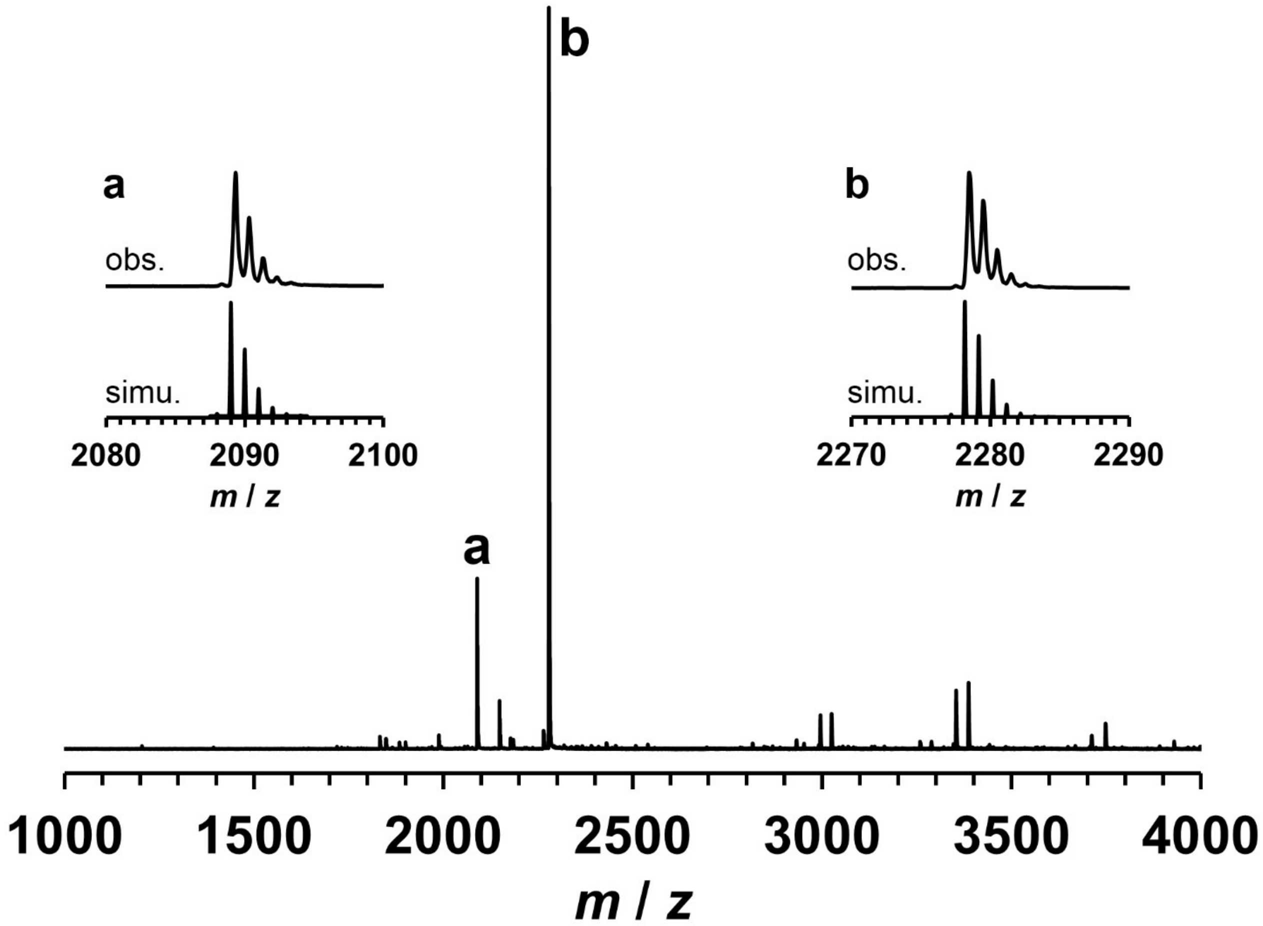

peak	ion	*m* / *z*
a	$\{(Et_4N)_6Mn_6O_6(V_4O_{13})_2(CH_3CO_2)\}^+$	2089.3
b	$\{(Et_4N)_7Mn_6O_6(V_4O_{13})_2(CH_3CO_2)_2\}^+$	2278.2

Figure S1. Positive-ion CSI-MS spectrum of **1(MeCO$_2$)** in acetonitrile. The table shows the assignment of peaks.

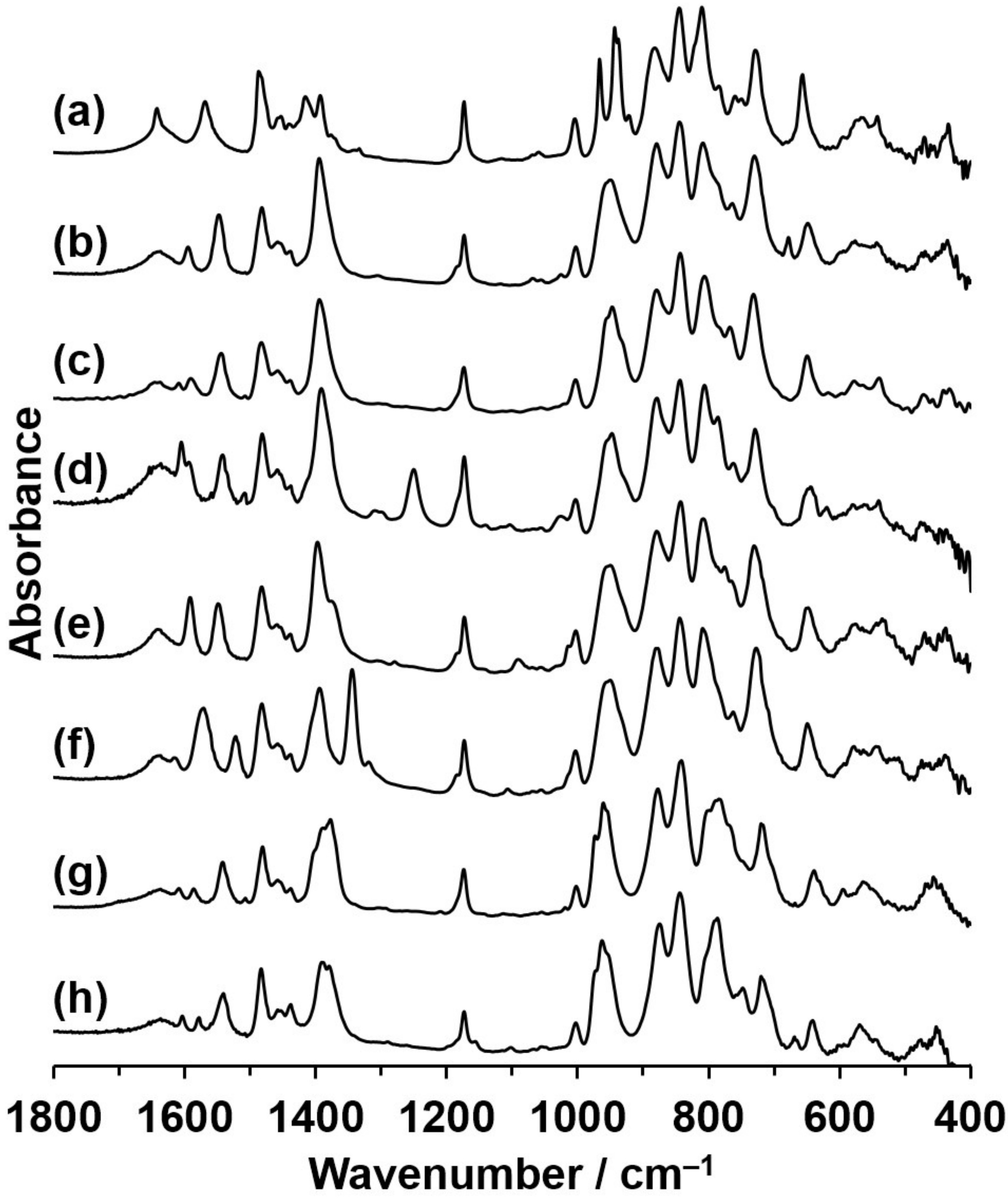

Figure S2. IR spectra of (a) **1(MeCO$_2$)**, (b) **1(PhCO$_2$)**, (c) **1(*p*-MePhCO$_2$)**, (d) **1(*p*-MeOPhCO$_2$)**, (e) **1(*p*-ClPhCO$_2$)**, (f) **1(*p*-NO$_2$PhCO$_2$)**, (g) **2(*p*-MePhCO$_2$)**, and (h) **2(*o*-MePhCO$_2$)**.

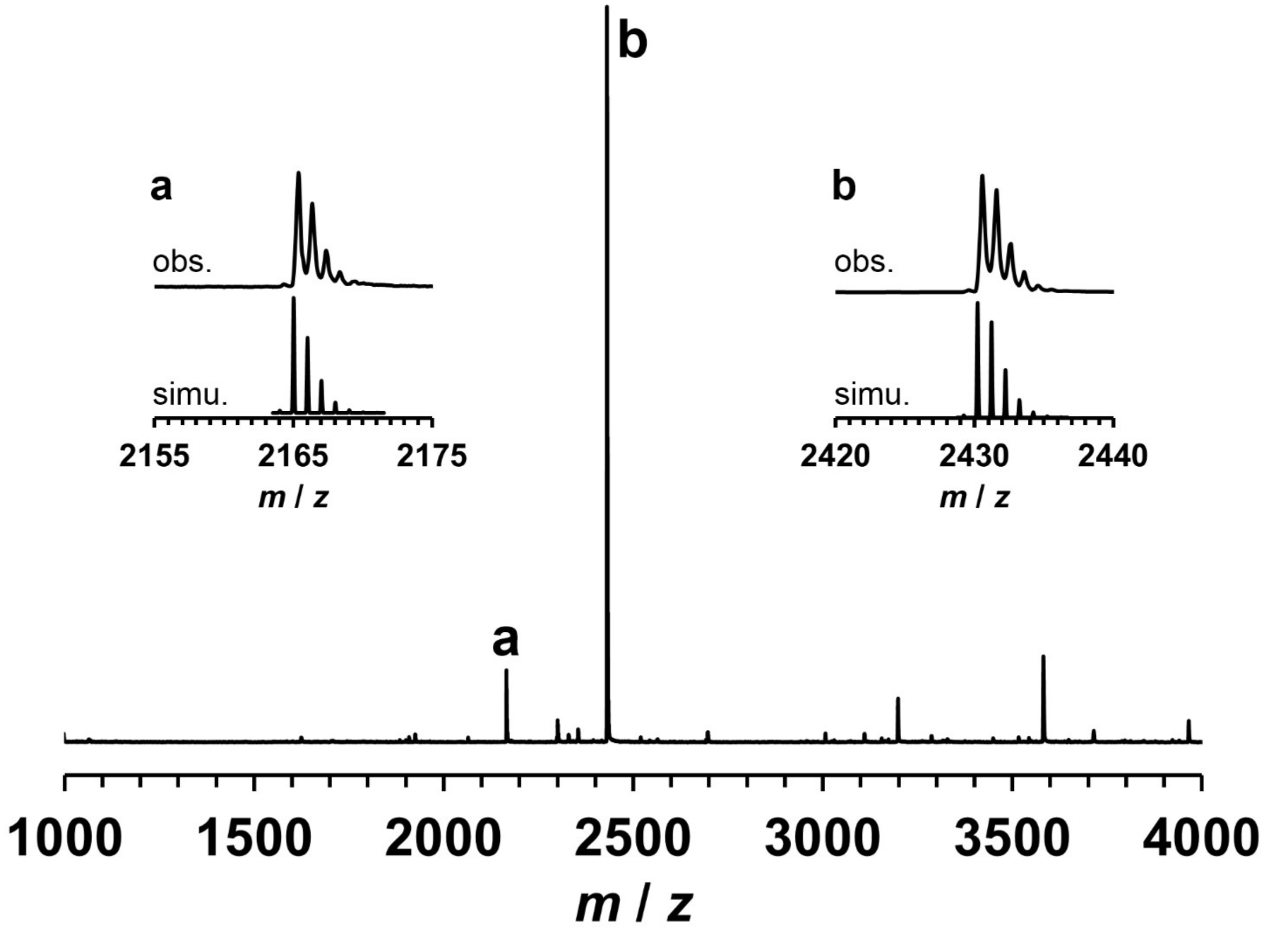

peak	ion	*m* / *z*
a	$\{(Et_4N)_6Mn_6O_6(V_4O_{13})_2(CH_3C_6H_4CO_2)\}^+$	2165.0
b	$\{(Et_4N)_7Mn_6O_6(V_4O_{13})_2(CH_3C_6H_4CO_2)_2\}^+$	2430.2

Figure S3. Positive-ion CSI-MS spectrum of **1(*p*-MePhCO$_2$)** in acetonitrile. The table shows the assignment of peaks.

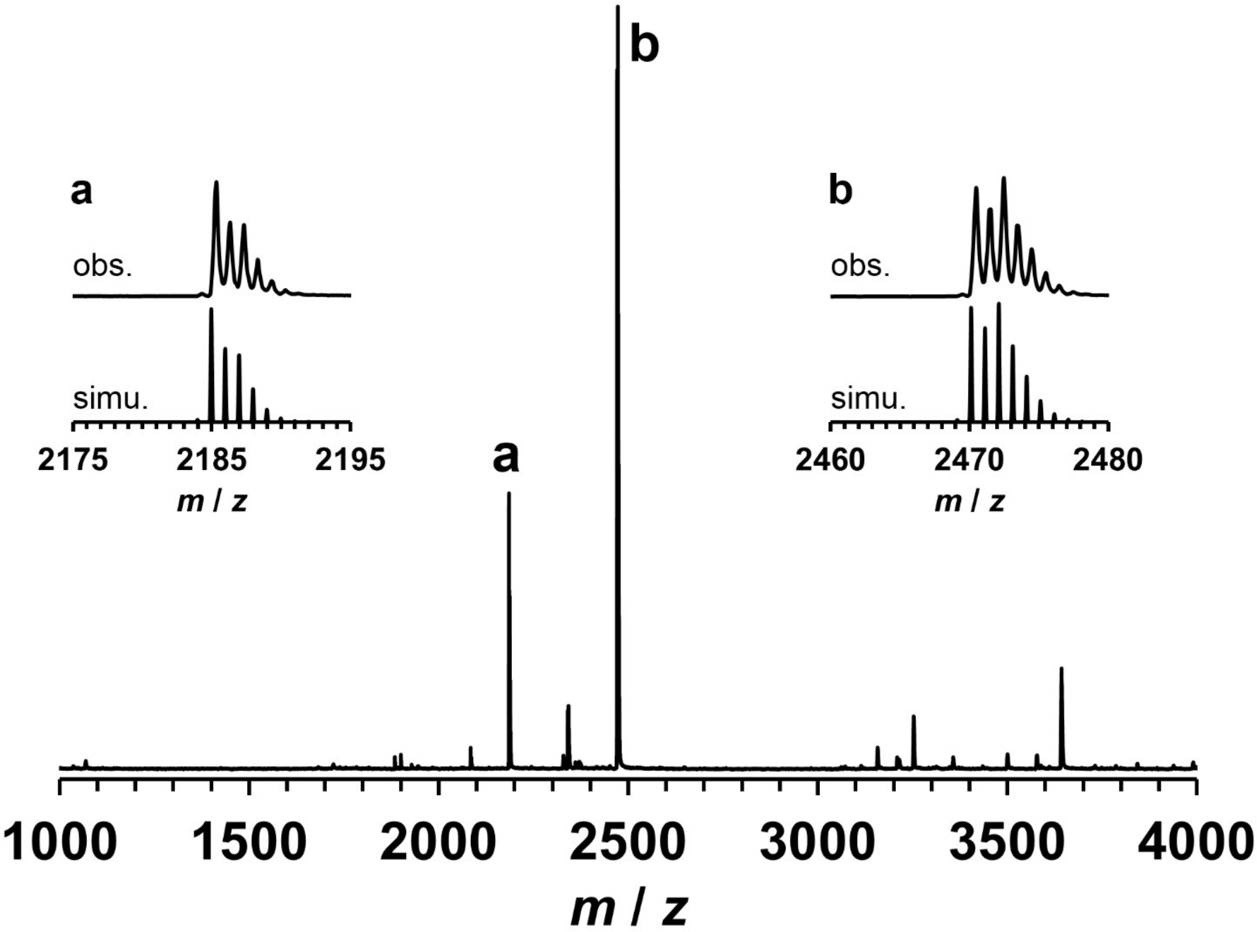

peak	ion	*m* / *z*
a	$\{(Et_4N)_6Mn_6O_6(V_4O_{13})_2(ClC_6H_4CO_2)\}^+$	2185.0
b	$\{(Et_4N)_7Mn_6O_6(V_4O_{13})_2(ClC_6H_4CO_2)_2\}^+$	2470.1

Figure S4. Positive-ion CSI-MS spectrum of **1(*p*-ClPhCO$_2$)** in acetonitrile. The table shows the assignment of peaks.

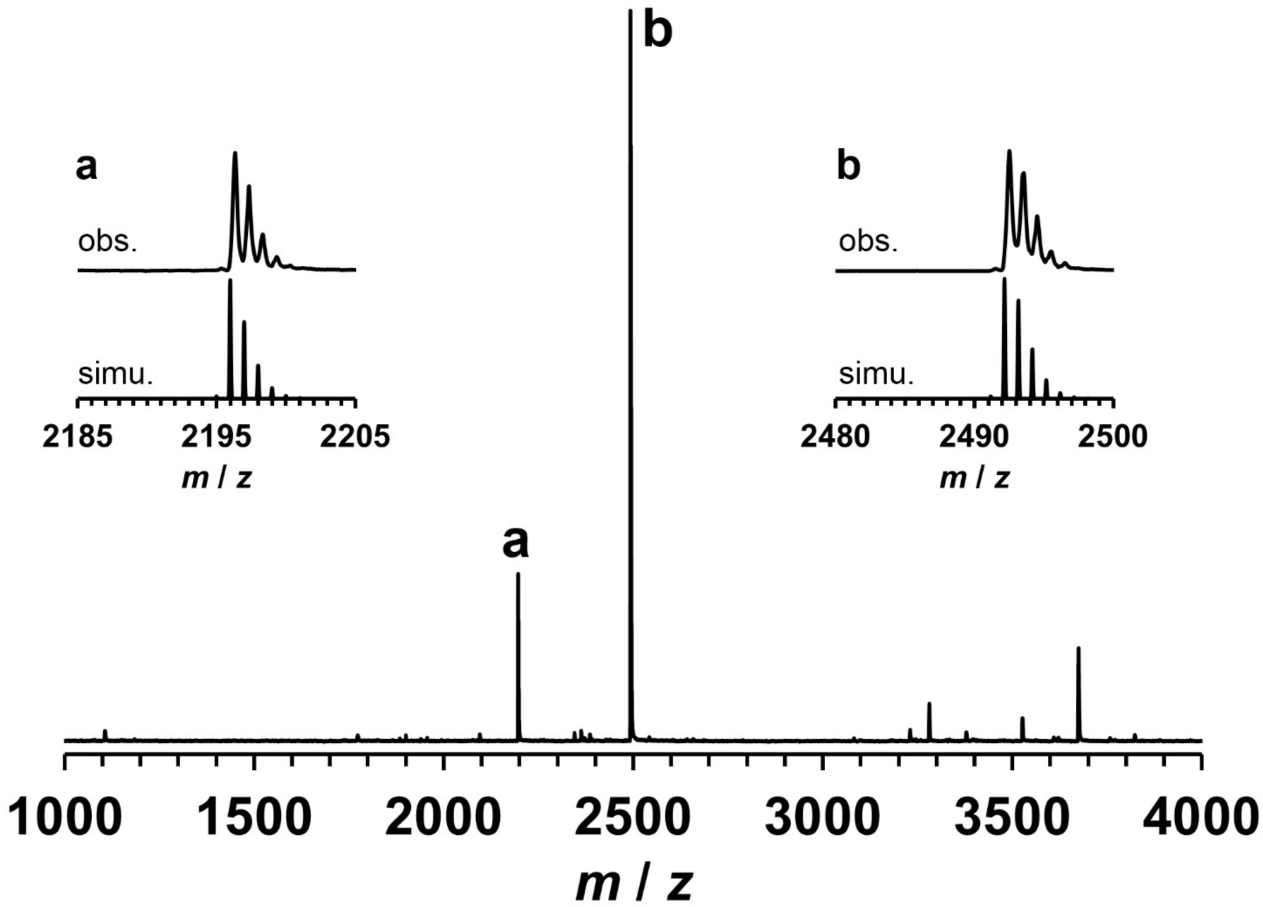

peak	ion	*m* / *z*
a	$\{(Et_4N)_6Mn_6O_6(V_4O_{13})_2(NO_2C_6H_4CO_2)\}^+$	2196.0
b	$\{(Et_4N)_7Mn_6O_6(V_4O_{13})_2(NO_2C_6H_4CO_2)_2\}^+$	2492.2

Figure S5. Positive-ion CSI-MS spectrum of **1(*p*-NO$_2$PhCO$_2$)** in acetonitrile. The table shows the assignment of peaks.

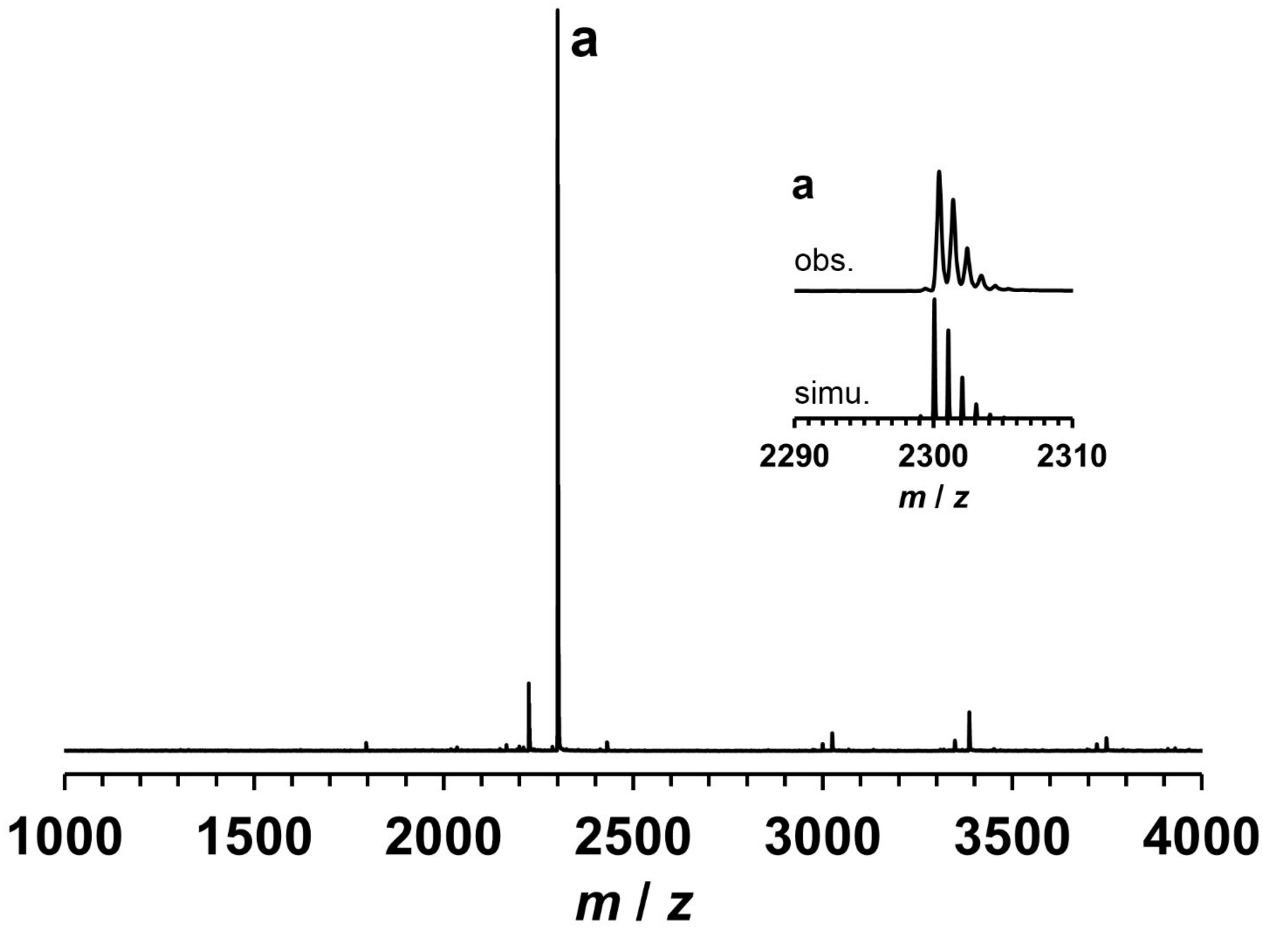

peak	ion	*m* / *z*
a	$\{(Et_4N)_6Mn_6O_6(V_4O_{13})_2(CH_3C_6H_4CO_2)_2\}^+$	2196.0

Figure S6. Positive-ion CSI-MS spectrum of **2(*o*-MePhCO$_2$)** in acetonitrile. The table shows the assignment of peaks.

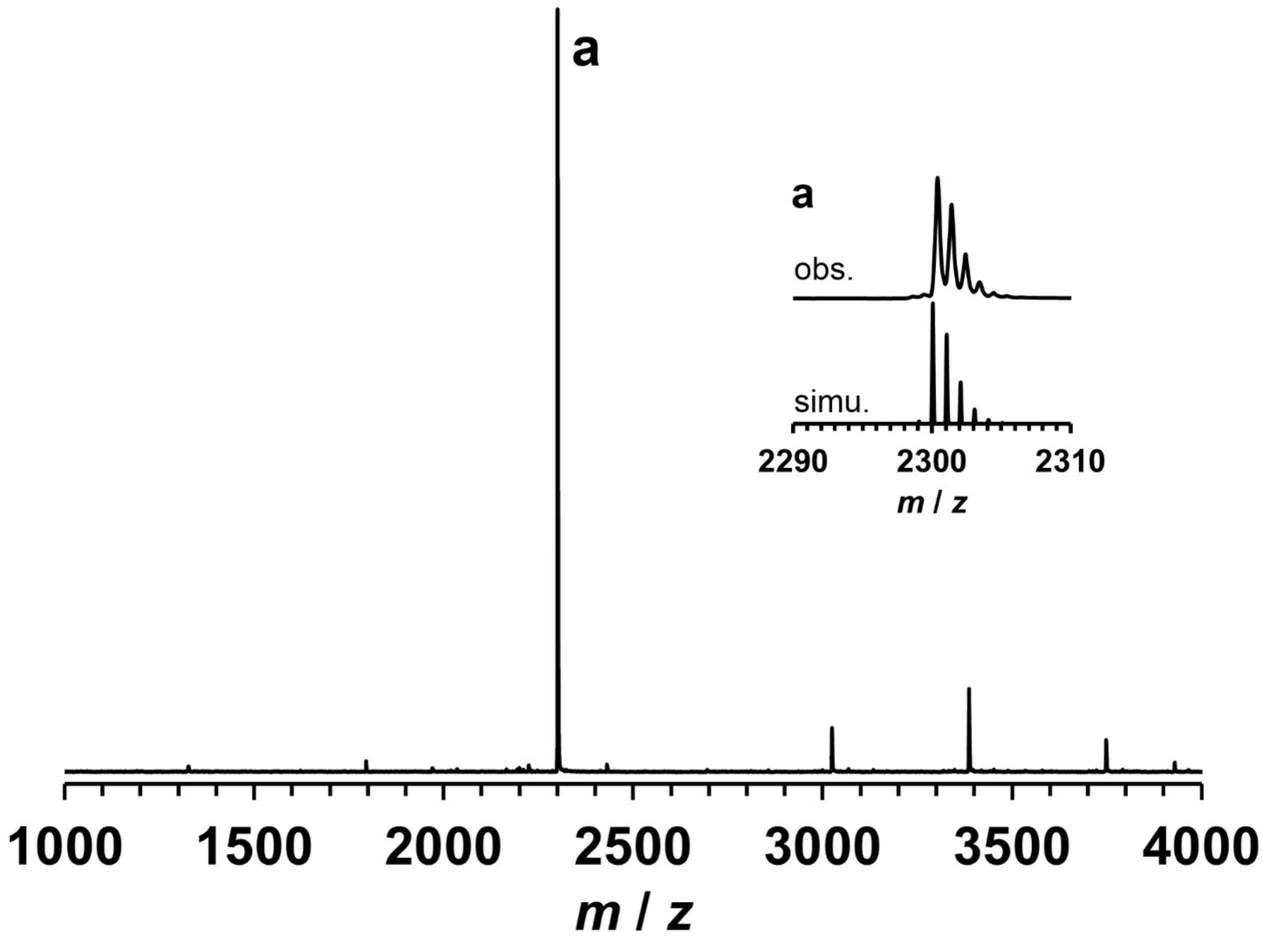

peak	ion	*m* / *z*
a	$\{(Et_4N)_6Mn_6O_6(V_4O_{13})_2(CH_3C_6H_4CO_2)_2\}^+$	2196.0

Figure S7. Positive-ion CSI-MS spectrum of **2(*p*-MePh)** in acetonitrile. The table shows the assignment of peaks.

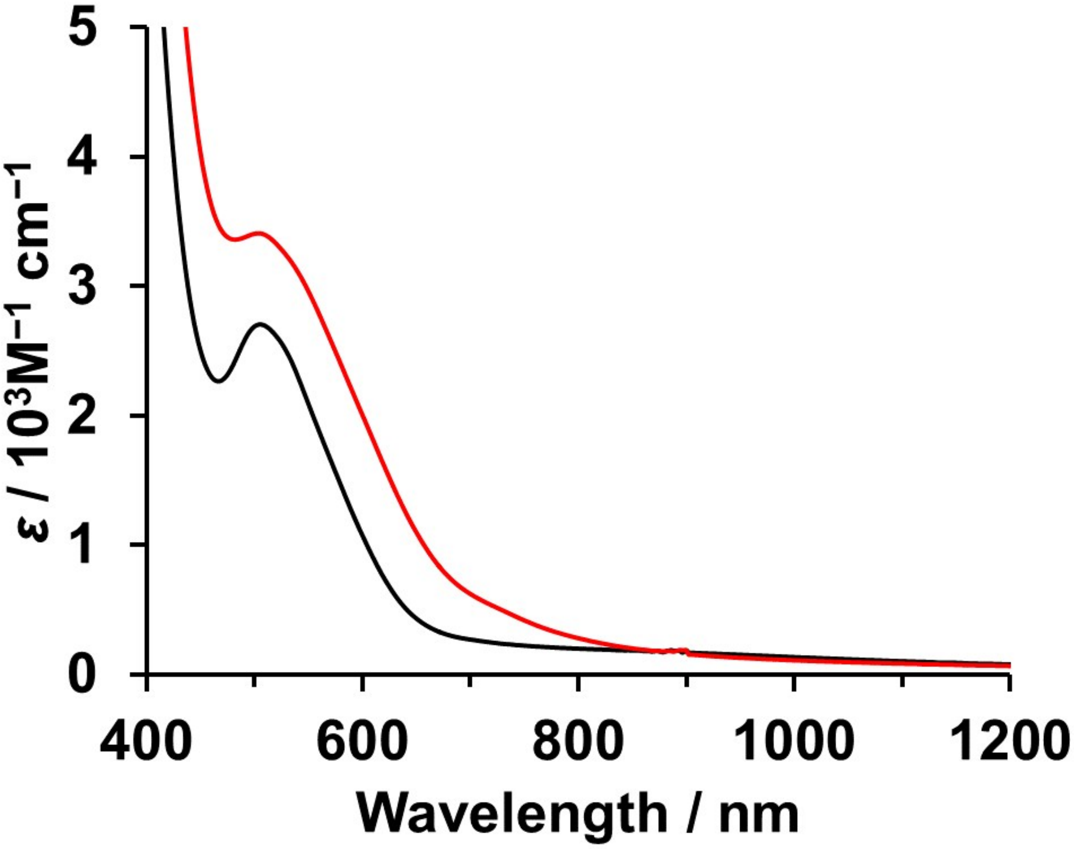

Figure S8. UV-Vis-NIR spectra of **1(*p*-MePhCO$_2$)** (black line) and **2(*p*-MePhCO$_2$)** (red line) in acetonitrile (2.0×10^{-5} M).

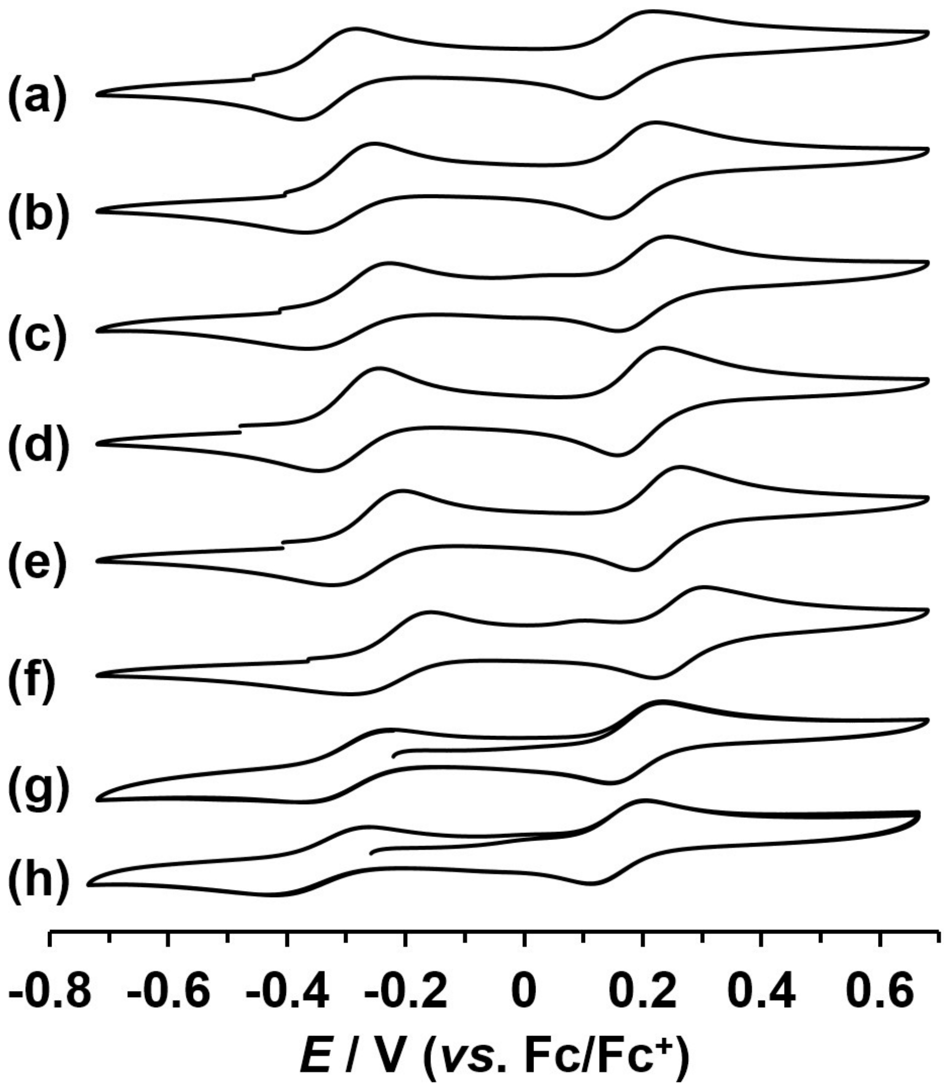

Figure S9. Cyclic voltammograms of (a) **1($MeCO_2$)**, (b) **1(*p*-$MeOPhCO_2$)**, (c) **1($PhCO_2$)**, (d) **1(*p*-$MePhCO_2$)**, (e) **1(*p*-$ClPhCO_2$)**, (f) **1(*p*-NO_2PhCO_2)**, (g) **2(*p*-$MePhCO_2$)**, and **2(*o*-$MePhCO_2$)** in acetonitrile. Scan rate was 100 mV/s. The working electrode was glassy carbon and the reference electrode was the Ag/Ag^+ electrode. The supporting electrolyte was (*n*-Bu_4N)PF_6.

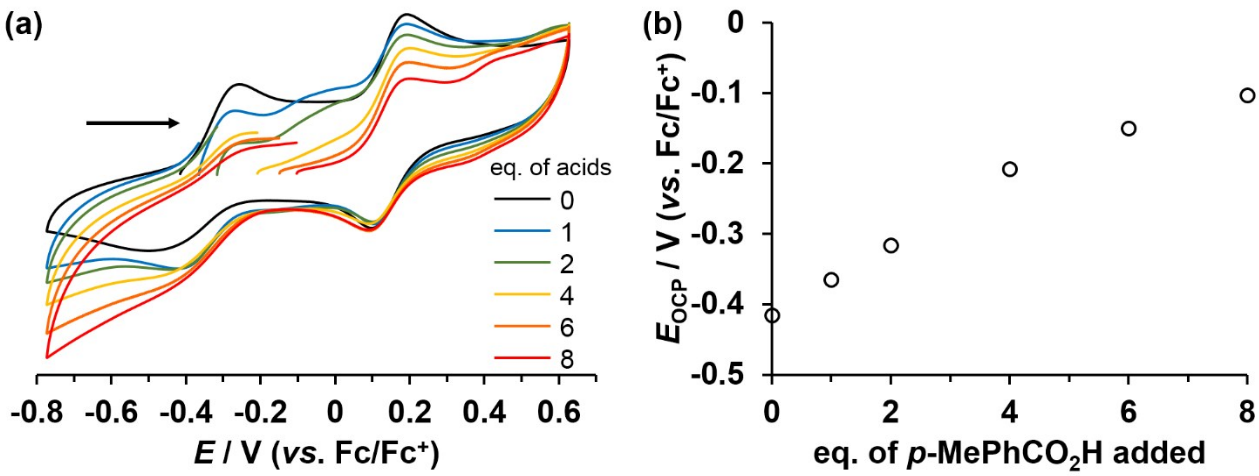

Figure S10. (a) Cyclic voltammograms of **1(*p*-MePhCO$_2$)** in acetonitrile in the presence of 0, 1, 2, 4, 6, 8 eq. of *p*-MePhCO$_2$H. (b) Plots of the eq. of *p*-MePhCO$_2$H added to **1(*p*-MePhCO$_2$)** versus the observed open circuit potential (E_{OCP}) of **1(*p*-MePhCO$_2$)** in the presence of *p*-MePhCO$_2$H.

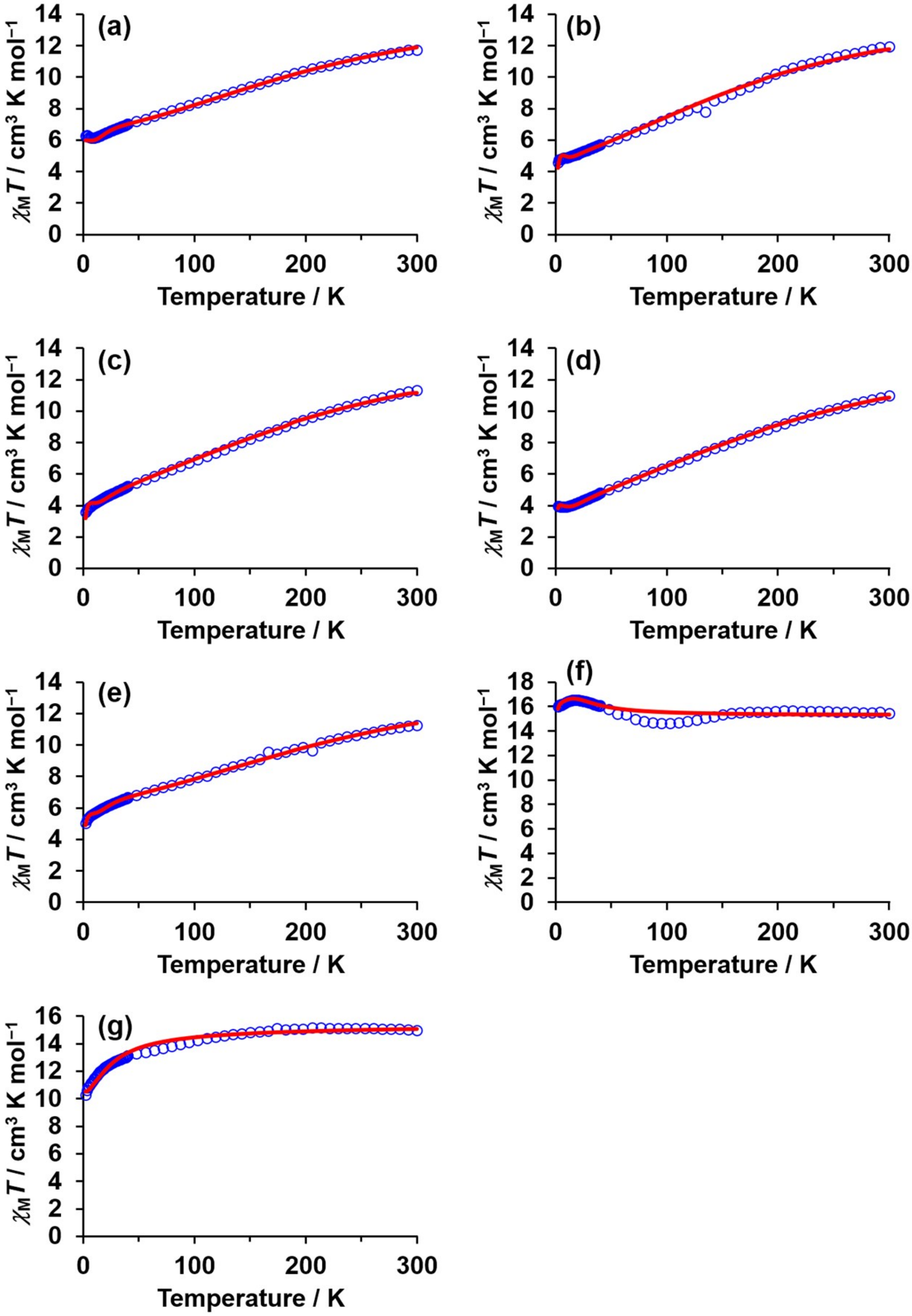

Figure S11. Temperature dependence of $\chi_M T$ values of (a) **1(MeCO$_2$)**, (b) **1(PhCO$_2$)**, (c) **1(*p*-ClPhCO$_2$)**, (d) **1(*p*-MePhCO$_2$)**, (e) **1(*p*-NO$_2$PhCO$_2$)**, (f) **2(*p*-MePhCO$_2$)**, and (g) **2(*o*-MePhCO$_2$)** in the temperature range of 2–300 K under the magnetic field of 1000 Oe. Solid lines represents the best fits.

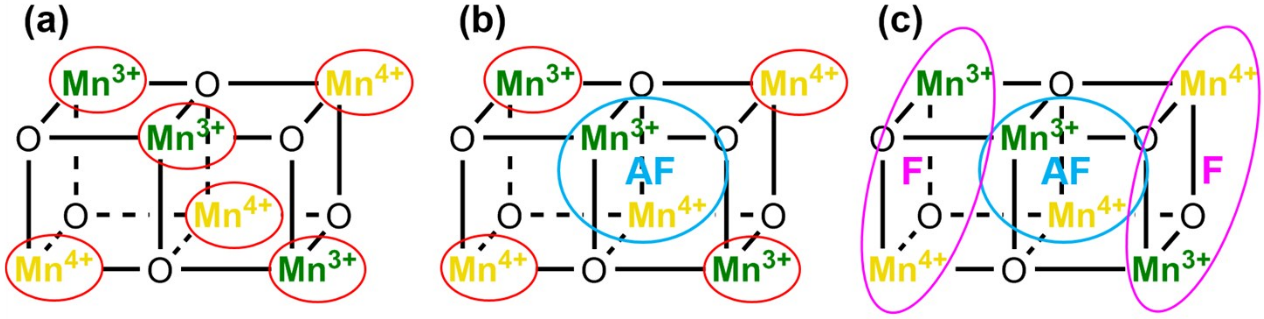

Figure S12. Magnetic coupling scheme for (a) the **2(RCO$_2$)** complexes at 300 K, (b) **2(*o*-MePhCO$_2$)** at 2 K, and (c) **2(*p*-MePhCO$_2$)** at 2 K.

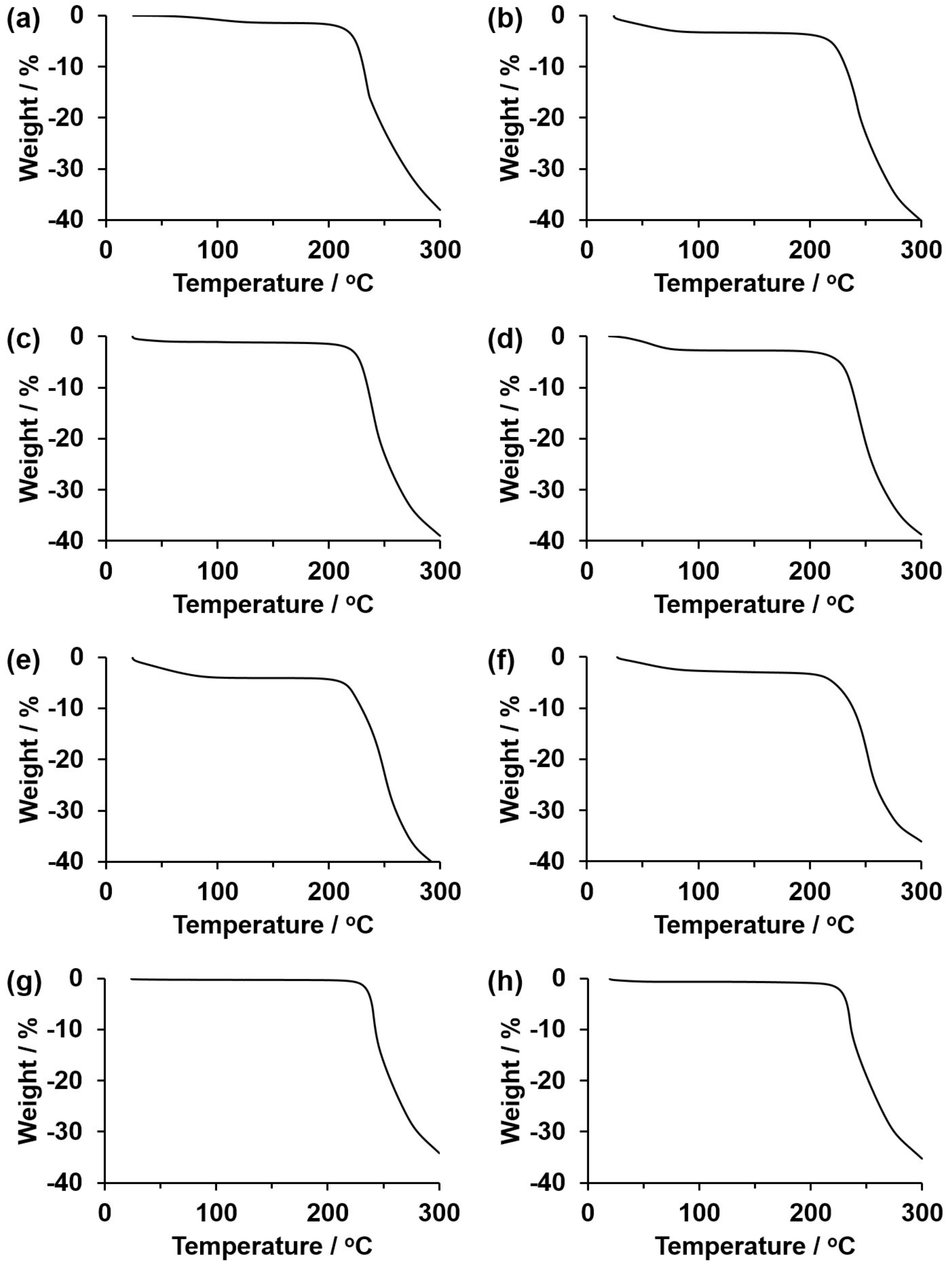

Figure S13. Thermogravimetric analysis of (a) **1(MeCO$_2$)**, (b) **1(PhCO$_2$)**, (c) **1(*p*-MePhCO$_2$)**, (d) **1(*p*-MeOPhCO$_2$)**, (e) **1(*p*-ClPhCO$_2$),** (f) **1(*p*-NO$_2$PhCO$_2$)**, (g) **2(*p*-MePhCO$_2$)**, and (h) **2(*o*-MePhCO$_2$)**.

Additional References

S1 C. M. Tourné, G. F. Tourné, S. A. Malik and T. J. R. Weakley, *J. Inorg. Nucl. Chem.*, 1970, **32**, 3875–3890.

S2 D. K. Lyon, W. K. Miller, T. Novet, P. J. Domaille, E. Evitt, D. C. Johnson and R. G. Finke, *J. Am. Chem. Soc.*, 1991, **113**, 7209–7221.

S3 R. Murugesan, T. Jeyabalan, P. Sami and A. Shunmugasundaram, *Proc. Indian Acad. Sci. Chem. Sci.*, 1998, **110**, 7–19.

S4 X.-Y. Zhang, M. T. Pope, M. R. Chance and G. B. Jameson, *Polyhedron*, 1995, **14**, 1381–1392.

S5 J. J. Cowan, A. J. Bailey, R. A. Heintz, B. T. Do, K. I. Hardcastle, C. L. Hill and I. A. Weinstock, *Inorg. Chem.*, 2001, **40**, 6666–6675.

S6 C. Pichon, P. Mialane, E. Rivière, G. Blain, A. Dolbecq, J. Marrot, F. Sécheresse and C. Duboc, *Inorg. Chem.*, 2007, **46**, 7710–7712.

S7 Y.-F. Song, D.-L. Long, S. E. Kelly and L. Cronin, *Inorg. Chem.*, 2008, **47**, 9137–9139.

S8 G. Izzet, E. Ishow, J. Delaire, C. Afonso, J.-C. Tabet and A. Proust, *Inorg. Chem.*, 2009, **48**, 11865–11870.

S9 H. Karoui and C. Ritchie, *Dalton Trans.*, 2016, **45**, 18838–18841.

S10 E. Al-Sayed, A. Blazevic, A. Roller and A. Rompel, *Chem. Eur. J.*, 2015, **21**, 17800–17807.

S11 S. Vanhaecht, T. Quanten and T. N. Parac-Vogt, *Inorg. Chem.*, 2017, **56**, 3095–3101.

S12 C. Ritchie and G. Bryant, *Dalton Trans.*, 2015, **44**, 20826–20829.

S13 R. E. Schreiber, H. Cohen, G. Leitus, S. G. Wolf, A. Zhou, L. Que and R. Neumann, *J. Am. Chem. Soc.*, 2015, **137**, 8738–8748.

S14 R. Sato, K. Suzuki, T. Minato, M. Shinoe, K. Yamaguchi and N. Mizuno, *Chem. Commun.*, 2015, **51**, 4081–4084.

S15 J. Jia, P. Ma, P. Zhang, D. Zhang, Y. Niu, J. Wang, C. Zhang and J. Niu, *Inorg. Chem.*, 2017, **56**, 10131–10134.

S16 C. M. Flynn and M. T. Pope, *J. Am. Chem. Soc.*, 1970, **92**, 85–90.

S17 C. M. Flynn and M. T. Pope, *Inorg. Chem.*, 1970, **9**, 2009–2014.

S18 W. Guo, J. Bacsa, J. van Leusen, K. P. Sullivan, H. Lv, P. Kögerler and C. L. Hill, *Inorg. Chem.*, 2015, **54**, 10604–10609.

S19 K. Kastner, J. Forster, H. Ida, G. N. Newton, H. Oshio and C. Streb, *Chem. Eur. J.*, 2015, **21**, 7686–7689.

S20 X. Zhang and M. T. Pope, *J. Mol. Catal. A Chem.*, 1996, **114**, 201–208.

S21 J.-H. Son and W. H. Casey, *Dalton Trans.*, 2013, **42**, 13339–13342.

S22 M. Xu, F. Li, T. Wang and L. Xu, *Inorg. Chem. Commun.*, 2018, **94**, 123–126.

S23 P. A. Abramov, M. M. Akhmetova, T. E. Romanova, A. S. Bogomyakov, M. V. Fedin and M. N. Sokolov, *Inorg. Chim. Acta*, 2018, **473**, 268–274.

S24 C. M. Tourné, G. F. Tourné and F. Zonnevijlle, *J. Chem. Soc., Dalton Trans.*, 1991, **22**, 143–155.

S25 X.-Y. Zhang, C. J. O'Connor, G. B. Jameson and M. T. Pope, *Inorg. Chem.*, 1996, **35**, 30–34.

S26 U. Kortz, S. Isber, M. H. Dickman and D. Ravot, *Inorg. Chem.*, 2000, **39**, 2915–2922.

S27 I. M. Mbomekalle, B. Keita, M. Nierlich, U. Kortz, P. Berthet and L. Nadjo, *Inorg. Chem.*, 2003, **42**, 5143–5152.

S28 P. Mialane, C. Duboc, J. Marrot, E. Rivière, A. Dolbecq and F. Sécheresse, *Chem. Eur. J.*, 2006, **12**, 1950–1959.

S29 J. Bai, F. Li, Z. Sun, Z. Jin and L. Xu, *Inorg. Chim. Acta*, 2017, **458**, 1–7.

S30 P.-E. Car, B. Spingler, S. Weyeneth, J. Patscheider and G. R. Patzke, *Polyhedron*, 2013, **52**, 151–158.

S31 H. Ichida, K. Nagai, Y. Sasaki and M. T. Pope, *J. Am. Chem. Soc.*, 1989, **111**, 586–591.

S32 U. Kortz and S. Matta, *Inorg. Chem.*, 2001, **40**, 815–817.

S33 P. Mialane, J. Marrot, E. Rivière, J. Nebout and G. Hervé, *Inorg. Chem.*, 2001, **40**, 44–48.

S34 D. Drewes, M. Piepenbrink and B. Krebs, *J. Clust. Sci.*, 2006, **17**, 361–374.

S35 D. Shevchenko, P. Huang, V. V. Bon, M. F. Anderlund, V. N. Kokozay, S. Styring and A. Thapper, *Dalton Trans.*, 2013, **42**, 5130–5139.

S36 R. Al-Oweini, B. S. Bassil, T. Palden, B. Keita, Y. Lan, A. K. Powell and U. Kortz, *Polyhedron*, 2013, **52**, 461–466.

S37 D. Dutta, A. D. Jana, M. Debnath, G. Mostafa, R. Clérac, J. G. Tojal and M. Ali, *Eur. J. Inorg. Chem.*, 2010, **2010**, 5517–5522.

S38 C. J. Gomez-Garcia, J. J. Borras-Almenar, E. Coronado and L. Ouahab, *Inorg. Chem.*, 1994, **33**, 4016–4022.

S39 Xiao-Yan Zhang, G. B. Jameson, C. J. O'Connor and M. T. Pope, *Polyhedron*, 1996, **15**, 917–922.

S40 H.-H. Wu, S. Yao, Z.-M. Zhang, Y.-G. Li, Y. Song, Z.-J. Liu, X.-B. Han and E.-B. Wang, *Dalton Trans.*, 2013, **42**, 342–346.

S41 R. Sato, K. Suzuki, T. Minato, K. Yamaguchi and N. Mizuno, *Inorg. Chem.*, 2016, **55**, 2023–2029.

S42 Z.-G. Han, H.-X. Zhang, D.-S. Zhang, C.-N. Liu, R. Zheng, G.-B. Xia and X.-X. Wang, *Inorg. Chem.*, 2016, **55**, 12488–12491.

S43 L. Y. Fan, Z. G. Lin, J. Cao and C. W. Hu, *Inorg. Chem.*, 2016, **55**, 2900–2908.

S44 B. Schwarz, J. Forster, M. K. Goetz, D. Yücel, C. Berger, T. Jacob and C. Streb, *Angew. Chem., Int. Ed.*, 2016, **55**, 6329–6333.

S45 M. Ibrahim, E. Moreno-Pineda, T. Bergfeldt, C. Anson and A. Powell, *Materials*, 2018, **11**, 155–167.

S46 R. Gupta, I. Khan, F. Hussain, A. M. Bossoh, I. M. Mbomekallé, P. de Oliveira, M. Sadakane, C. Kato, K. Ichihashi, K. Inoue and S. Nishihara, *Inorg. Chem.*, 2017, **56**, 8759–8767.

S47 S.-L. Zhu, X. Xu, S. Ou, M. Zhao, W.-L. He and C.-D. Wu, *Inorg. Chem.*, 2016, **55**, 7295–7300.

S48 S. Das, A. Misra and S. Roy, *New J. Chem.*, 2016, **40**, 994–1003.

S49 X. Fang and P. Kögerler, *Chem. Commun.*, 2008, 3396–3398.

S50 S. G. Mitchell, S. Khanra, H. N. Miras, T. Boyd, D.-L. Long and L. Cronin, *Chem. Commun.*, 2009, 2712–2714.

S51 N. Jiang, F. Li, L. Xu, Y. Li and J. Li, *Inorg. Chem. Commun.*, 2010, **13**, 372–375.

S52 S. G. Mitchell, P. I. Molina, S. Khanra, H. N. Miras, A. Prescimone, G. J. T. Cooper, R. S. Winter, E. K. Brechin, D.-L. Long, R. J. Cogdell and L. Cronin, *Angew. Chem., Int. Ed.*, 2011, **50**, 9154–9157.

S53 M. Martin-Sabi, R. S. Winter, C. Lydon, J. M. Cameron, D.-L. Long and L. Cronin, *Chem. Commun.*, 2016, **52**, 919–921.

S54 H. Xue, J.-W. Zhao, R. Pan, B.-F. Yang, G.-Y. Yang and H.-S. Liu, *Chem. Eur. J.*, 2016, **22**, 12322–12331.

S55 X. Fang and P. Kögerler, *Angew. Chem., Int. Ed.*, 2008, **47**, 8123–8126.

S56 X. Fang, P. Kögerler, M. Speldrich, H. Schilder and M. Luban, *Chem. Commum.*, 2012, **48**, 1218–1220.

S57 N. H. Nsouli, A. H. Ismail, I. S. Helgadottir, M. H. Dickman, J. M. Clemente-Juan and U. Kortz, *Inorg. Chem.*, 2009, **48**, 5884–5890.

S58 S. G. Mitchell, H. N. Miras, D.-L. Long and L. Cronin, *Inorg. Chim. Acta*, 2010, **363**, 4240–4246.

S59 R. Al-Oweini, U. Kortz, M. Itani, B. S. Bassil and D. B. Emiroğlu, *Acta Crystallogr., Sect. C*, 2018, **74**, 1390–1394.

S60 J. Thiel, P. I. Molina, M. D. Symes and L. Cronin, *Cryst. Growth Des.*, 2012, **12**, 902–908.

S61 Q. Wu, Y.-G. Li, Y.-H. Wang, E.-B. Wang, Z.-M. Zhang and R. Clérac, *Inorg. Chem.*, 2009, **48**, 1606–1612.

S62 X. Fang and M. Luban, *Chem. Commun.*, 2011, **47**, 3066–3068.

S63 D. Zhang, F. Cao, P. Ma, C. Zhang, Y. Song, Z. Liang, X. Hu, J. Wang and J. Niu, *Chem. Eur. J.*, 2015, **21**, 17683–17690.

S64 A. Haider, M. Ibrahim, B. S. Bassil, A. M. Carey, A. N. Viet, X. Xing, W. W. Ayass, J. F. Miñambres, R. Liu, G. Zhang, B. Keita, V. Mereacre, A. K. Powell, K. Balinski, A. T. N'Diaye, K. Küpper, H.-Y. Chen, U. Stimming and U. Kortz, *Inorg. Chem.*, 2016, **55**, 2755–2764.

S65 B. S. Bassil, M. Ibrahim, R. Al-Oweini, M. Asano, Z. Wang, J. van Tol, N. S. Dalal, K.-Y. Choi, R. Ngo Biboum, B. Keita, L. Nadjo and U. Kortz, *Angew. Chem., Int. Ed.*, 2011, **50**, 5961–5964.

S66 T. Minato, K. Suzuki, K. Yamaguchi and N. Mizuno, *Angew. Chem., Int. Ed.*, 2016, **55**, 9630–9633.

S67 X. Fang, P. Kögerler, Y. Furukawa, M. Speldrich and M. Luban, *Angew. Chem., Int. Ed.*, 2011, **50**, 5212–5216.